Table of content

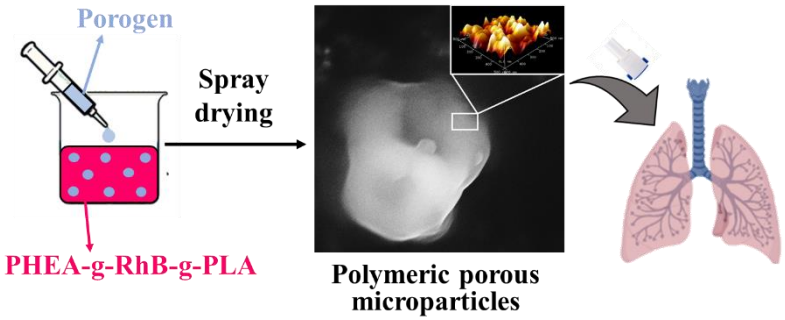

Polymeric microparticles with tunable porosity were produced by spray-drying (SD) by using PHEA-g-RhB-g-PLA graft copolymer and ammonium bicarbonate as porogen agent, and were proposed as inhalable powder for pulmonary drug delivery.

Inhalable polymeric microparticles as pharmaceutical porous powder for drug administration

Emanuela F. Craparo[1,2], Marta Cabibbo[1], Salvatore Emanuele Drago[1], Luca Casula[3], Francesco Lai[3], Gennara Cavallaro[1,2,4]*

[1]Lab of Biocompatible Polymers, Department of Biological, Chemical and Pharmaceutical Sciences and Technologies (STEBICEF), University of Palermo, Via Archirafi 32, Palermo, 90123, Italy

[2]Consorzio Interuniversitario Nazionale per la Scienza e Tecnologia dei Materiali (INSTM) of Palermo.

[3] Department of Life and Environmental Sciences, University of Cagliari, Via Ospedale, 72, 09124 Cagliari, Italy;

[4]Advanced Technology and Network Center (ATeN Center), University of Palermo, Palermo 90133, Italy.

Emanuela Fabiola Craparo: https://orcid.org/0000-0002-0503-9559
Marta Cabibbo: https://orcid.org/0000-0002-6244-9183
Luca Casula: https://orcid.org/0000-0001-9508-7222
Francesco Lai: https://orcid.org/0000-0003-4065-1572
Gennara Cavallaro: https://orcid.org/0000-0003-0585-6564

Abstract

In this work, the production of inhalable polymeric microparticles with modulable porosity is described. The starting polymeric material was the PHEA-g-RhB-g-PLA graft copolymer, which was suitably processed by spray drying (SD). Thanks to the addition of AB (weight percentage equal to 10 and 20 % with respect to the polymer) in the liquid feed, three biocompatible matrices were obtained with an increasing porosity in terms of pore volume (from 0.015 to 0.024 cc/g) and pore average diameter (from 1.942 to 3.060 nm), a decreasing tapped density values (from 0.75 to 0.50), and favorable aerosolization characteristics. These differences were highlighted also by a significant increase in the release of Rapamycin from the sample which showed the higher porosity (31.0 wt% after 24 hrs incubation) than the sample with the lowest porosity (14.9 wt%) in simulated lung fluid.

Keywords

α,β-Poly(N-2-hydroxyethyl)-D,L-aspartamide (PHEA), porous microparticles, pulmonary administration, Rapamycin.

Introduction

Modern research in the field of pharmaceutical technology is focused on the development of increasingly high-performance materials and, at the same time, innovative systems for the delivery of drugs obtained from the latter materials [1–3]. More precisely, the goal is to design and manufacture these systems for specific drugs whose bioavailability needs to be improved, such as traditional molecules, that might already be available in conventional dosage forms, or new drugs whose opportunity to be introduced on the market is precisely given by innovative systems that open the doors to new administration strategies [4,5].

As for the new materials, the technological needs can be satisfied by combining different components to obtain new mixed products, whose final characteristics are not only the sum of those of the individual components but also newly developed ones.

Among the recently developed pharmaceutical delivery systems, porous microparticles for the delivery of drugs to the lung still represent a field of great fervor [6–9]. The success of these systems is due to the fact that they have opened up the possibility for numerous drugs – with low and problematic bioavailability – to be exploited for the treatment of both local and systemic pathologies [10]. In particular, by suitably modulating size, density, surface properties, shape and dispersibility in the lung fluids, it is possible to promote their penetration (and therefore that of the encapsulated drug) into deep districts of the bronchial tree and to prolong their retention in the site of deposition, enhancing the drug release and its local pharmacological action or the specific accumulation of the drug in a cell type. On the other hand, when a systemic effect or an action in a district far from the lung tissue is needed, its passage in the aematic torrent might be adequately tuned [10,11].

Therefore, these systems have opened new treatment possibilities for lung diseases of a certain severity, such as chronic obstructive pulmonary disease (COPD) or asthma, whose chronic treatments are extremely complicated with oral or systemic therapies, as they are often accompanied by very serious adverse reactions [12].

To this extent, the production of porous microparticles starting from performing materials and their characterization using increasingly sophisticated techniques represents an extremely current and popular topic. Ammonium bicarbonate (AB) as porogen was successfully used to produce highly porous poly(lactic-co-glycolic acid) (PLGA) microparticles for pulmonary delivery of several kind of drugs such as Doxorubicin, budesonide and tiotropium [13–15];

likewise, large porous particles based of sodium hyaluronate (HA) were also obtained by spray drying (SD) and using AB for pulmonary delivery of meloxicam[16].

In this work, we described the production of polymeric microparticles (MPs) with tunable porosity starting from a biocompatible and versatile polymeric material and ammonium bicarbonate (AB) as porous agent, by means of the spray-drying (SD) process. Furthermore, the physical-chemical and technological characteristics of these particles, as well as the biocompatibility, were opportunely d evaluated to demonstrate that these particles can be proposed as potential carriers for pulmonary drug administration.

Materials and methods

Materials

Rhodamine B (RhB) and Polylactic acid (PLA), acetone, ethanol, methanol, dimethyl sulfoxide (DMSO), dimethyloformamide (DMF), carbonyldiimidazole (CDI), ammonium bicarbonate (AB), diethylamine (DEA) and dichloromethane, Dulbecco's phosphate-buffered saline (DPBS) were purchased from Sigma-Aldrich, (Italia). Rapamycin was purchased from Accel Pharmatech (NJ, USA). Spectra/Por 4 dialysis membranę Standard RC Tubing was purchased from Spectrum Laboratories Inc.

Microparticle production

Polymeric microparticles (MPs) were formulated by using Nano Spray Dryer B-90 HP from Buchi (Milan). A large diaphragm nebulizer was chosen and parameters such as temperature, air flow, pressure in the drying chamber, amount of atomized fluid (spray) and liquid flow through the pump have been kept constant, respectively equal to 60°C, 120 L/min, 25 hPa, 78%, and 40%.

MPs based on PHEA-g-RhB-g-PLA (no template, MP_NT) were obtained by spray drying (SD) a copolymer dispersion (1.5 or 3.0 % w/v) in an aceton:water mixture (39:1 v/v). To obtain the porous MPs, at the copolymer dispersion (1.5% w/v) AB was added to obtain a percentage weight between the porogen and the copolymer equal to 10 or 20 wt%, obtaining respectively MP_AB_10 and MP_AB_20 samples. Each final dispersion was filtered and spray dried, obtaining a powder, which was isolated by recovery from an electrostatic collector. In Table 1 the composition of the liquid feed for each MP sample is reported.

Table 1. Composition of the liquid feed for each MP sample.

Sample name	Composition of the liquid feed
MP_NT[a]	PHEA-RhB-PLA 1.5 % w/v[b]
MP_AB_10	PHEA-RhB-PLA 1.5 % w/v[b] + AB 0.15 wt % [c]
MP_AB_20	PHEA-RhB-PLA 1.5 % w/v[b] + AB 0.30 wt% [c]

[a] NT = no template

[b]copolymer weight percentage on the liquid feed.

[c]porogen weight percentage on the copolymer weight.

To obtain Rapamycin – loaded MPs, the drug was dissolved in the liquid feed, which composition for each sample is reported in Table 1, at a concentration equal to 0.08 % wt/vol, prior to SD. All the samples were recovered with at least 57 wt% yield with respect to the total components weight.

Surface analysis – porosity

Nitrogen specific surface area and porosity were determined by using a Brunauer-Emmet-Teller (BET) equipment from Quantachrome instrument, Autosorb iQ mp 8619, and ASiQwin. To carry out the analysis, each sample (~ 50 mg) was prior degassed for 6 hrs at 40°C and then subjected to N_2 at relative pressure P/P_0 between 0 and 1 at 77K. Obtained data were processed using the Multipoint BET and the Barrett, Joyner and Halenda (BJH) models. Each measurement was performed in triplicate.

Density

Tapped density of MPs was measured the syringe method[17]. In particular, each powder was filled in a 1 ml graduated syringe and the powder weight required to fill the syringe was recorded to calculate the bulk density. Then, the tapped density (ρ_{tapp}) was calculated from the volume value determined by tapping the syringe onto a level surface at a height of 2.5 cm, 100 times and repeating the tapping until the volume did not remain constant. Each measurement was performed in triplicate.

Theoretical aerodynamic particle diameter

The theoretical aerodynamic diameter (d_{aer}) was calculated by using the following equation [18,19].

$$\mathbf{d_{aer} = d_g \sqrt{\frac{\rho_{tapp}}{\chi \times \rho_0}}} \qquad \mathbf{(1)}$$

where d_{aer} = aerodynamic diameter, μm

d_g = geometric diameter, μm

ρ_{tapp} = tapped density, g/cm^3

χ = form factor (= 1 for spherical particles)

ρ_0 = unit density

Aerodynamic behavior

The aerodynamic behavior of each MP sample (MP_NT, MP_AB_10, MP_AB_20) was assessed using the dry powder inhaler (DPI) Breezhaler® attached to the Next Generation Impactor (NGI, Apparatus E, Eur. Ph 10th ed., Copley Scientific Ltd., Nottingham, UK) equipped with a pre-separator (PS) between the stage 1 and the induction port (IP), complying with the indication for DPI testing [18]. To prevent particle bouncing and re-entrainment, the PS and the impaction cups of each stage were coated with 1% (w/v) Tween 80 ® in ethanol prior to use, and allowed to dry for 30 min. The chosen coating solution has been reported as one of the most promising coating agents in terms of reproducibility and safe characteristics [20,21]. The flow rate was set to 90 L/min and checked with a flow meter (DFM3, Copley Scientific). Three capsules (size 3) manually filled (10 ± 0.1 mg) were discharged into the NGI for 2.7 s, in order to achieve an air passing volume of 4 L [22]. The deposited powder was then collected using a 50:50 (v/v) methanol:DMSO mixture and the copolymer fluorescence (due to the linked RhB) quantified by UV-Vis spectroscopy at λ = 562 nm, using a Synergy 4 multiplate reader (BioTek, Winooski, USA). For each sample, the experiment was repeated at least three times (3 capsules for each actuation) and the obtained data was analysed to give the emitted dose (ED; drug collected in the mouthpiece, IP, PS and impaction cups) and the ED% (ratio of the ED to the initial mass of sample tested). Moreover, the fine particle fraction (FPF%), defined as the mass percentage of the ED with an aerodynamic diameter less than 5.0 µm, was determined from interpolation of the cumulative aerodynamic diameter distribution curve between stage 1 and stage 2. The cumulative mass amount of each stage was plotted as a percentage of the recovered sample versus the cut-off diameter, not including the mass deposited in the induction port due to the unavailability of a precise upper size limit for particles deposited in this section. The mass median aerodynamic diameter (MMAD) of the particles – aerodynamic diameter at which 50% of the particles are larger and 50% are smaller – was then extrapolated from the graph according to the Eur. Ph. 10th ed., and the geometric standard deviation (GSD) value was determined. Moreover, the dispersibility index (DI) was calculated as the ratio of the MMAD to the theoretical d_{aer} obtained from Eq. 1, where low midair dispersion of the aerosols exiting the inhaler is represented by a large DI value [23,24].

Results

In this work, inhalable polymeric microparticles (MPs) with tunable porosity were produced by spray drying (SD) and proposed for pulmonary administration of drugs. The SD technique allows the modulation and optimization of the particle physical-chemical and technological properties (size, polydispersity index, density, morphology, surface area, porosity) and of the powder macroscopic characteristics (flowability, bulk and tapped density, etc.) by suitably adjusting the process variables and the characteristics of the feed fluid, i.e. the quali-quantitative composition [25].

The polymeric material chosen for the particle production was a graft copolymer obtained starting from the α,β-Poly(N-2-hydroxyethyl)-D,L-aspartamide (PHEA), functionalized in sequential steps with rhodamine (RhB) to make the polymer fluorescent, and with polylactic acid (PLA), to make PHEA-g-RhB insoluble in aqueous fluids [26–28]. The copolymer versatility for the realization of smart (from nano- to macro-) systems usable in various biomedical applications and the biocompatibility of particulate carriers made from PHEA-g-RhB-g-PLA (Fig. 1) were already been proven [29–31].

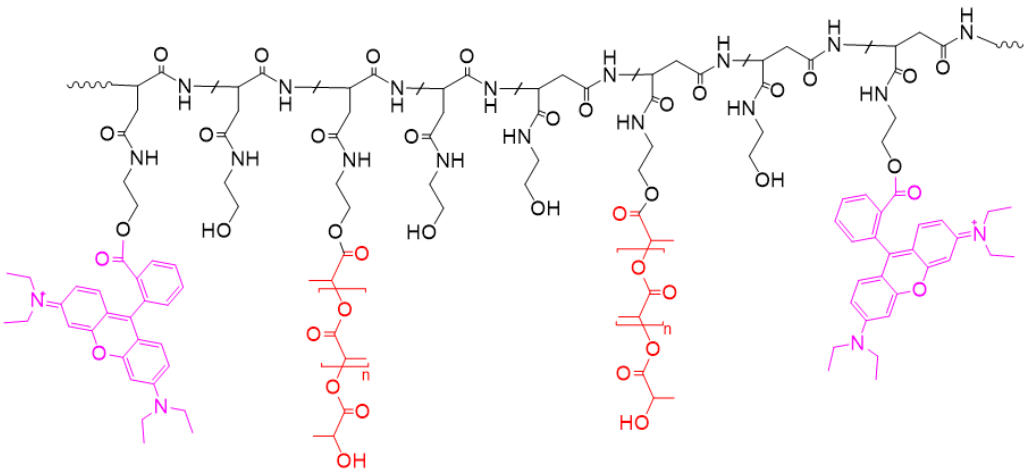

Fig. 1. The chemical structure of PHEA-g-RhB-g-PLA graft copolymer (n = 194) (PHEA mail backbone is reported in black, RhB in fuchsia, PLA chains in red).

The first step was to optimize the process variables of the SD process in order to obtain spherical microparticles (MPs) starting from the chosen copolymer [32]. The process involved spray drying of dispersions/solutions rather than surfactant-stabilised emulsions, providing for the production of excipient free MPs with proper physical properties such as amorphous state, porosity and low bulk density [17]. In our work, an acetone:water mixture 39:1 vol/vol

was chosen as liquid feed; therefore, the air flow in the drying chamber was fixed to 12 L/min, dehumidified and preheated at 60°C. Preliminary studies showed that 1.5 and 3.0 % w/v were the optimal values of PHEA-g-RhB-g-PLA concentrations in the feed fluid suitable to produce spherical MPs with low polydispersity by using a large mesh nebulizer. The recovered powders were named, respectively, MP_NT_1.5% and MP_NT_3% as a function of the copolymer final concentration in the liquid feed.

Figure 2 shows representative SEM images (see Supporting Information for experimental details) of the MPs samples; the average diameter with relative standard deviation, calculated using the ImageJ software on these images, are reported in Table 2, while the frequency size distribution in Fig. 3.

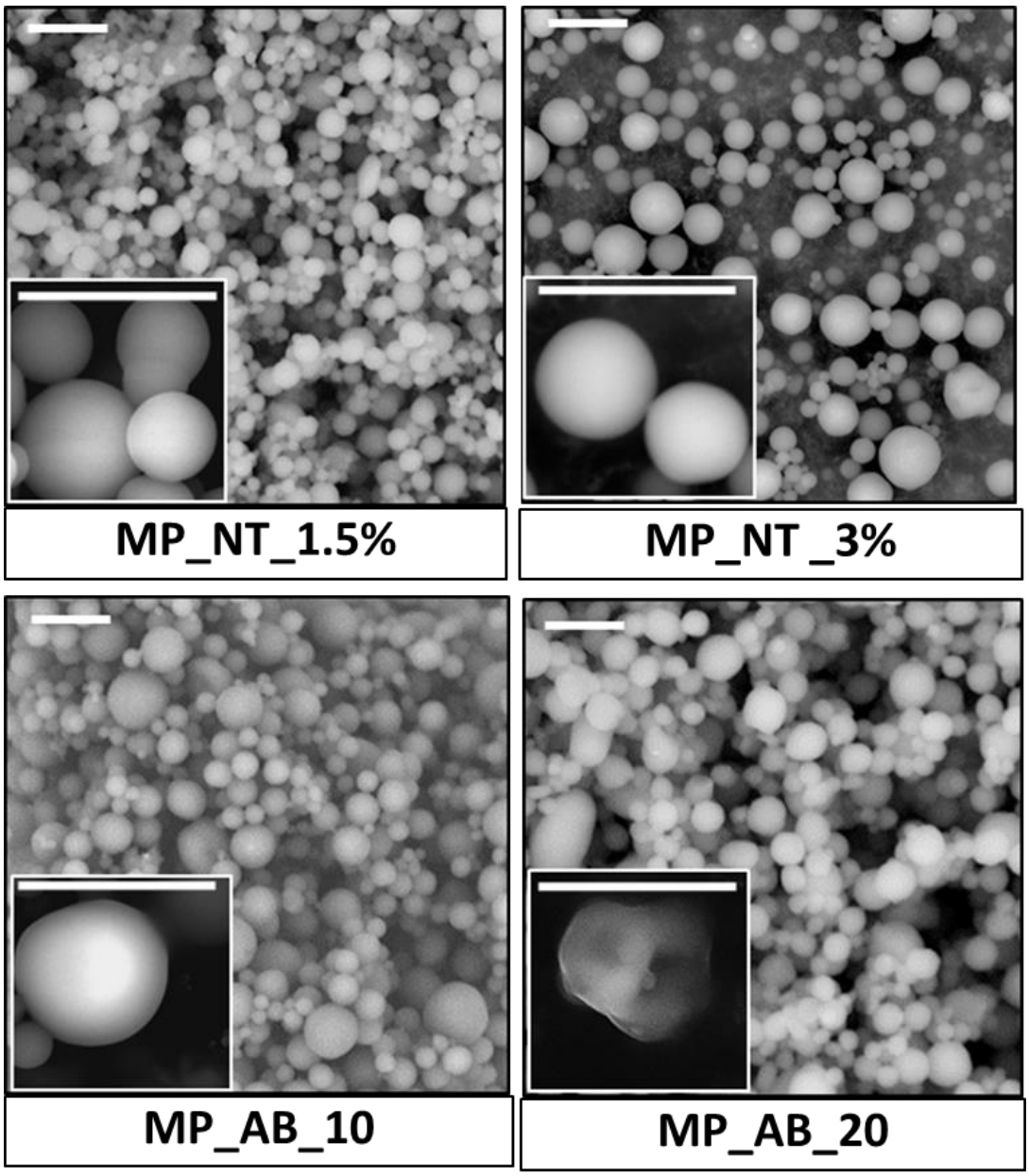

Fig. 2. Representative SEM images of MPs samples obtained at different copolymer concentrations (1.5% and 3% wt/vol) (MP_NT_1.5% and MP_NT_3% samples, respectively), and in the presence of 10 and 20 weight percentage of porogen on the copolymer weight (MP_AB_10 and MP_AB_20 samples, respectively), (big image: magnification = 8000x; inside image: 50,000x). Bar represents 4 μm.

Table 2. The mean geometric diameter (d_g) with standard deviation (S.D.) obtained by the ImageJ software (particle number > 1500) for the MP samples obtained by varying the copolymer concentration (MP_NT_1.5% and MP_NT_3%), and the AB weight percentage (MP_AB_10 and MP_AB_20).

Sample	d_g ±S.D. (μm)
MP_NT_3%	2.6 ± 0.7
MP_NT_1.5%	2.2 ± 0.3
MP_AB_10	3.6 ± 0.5
MP_AB_20	3.8 ± 0.5

As can be seen, as the copolymer concentration in the liquid feed increases (1.5% vs 3.0% wt/vol), the obtained particles showed larger mean diameter and higher dispersity. The effect of the copolymer concentration on particle size and polydispersity is highlighted on the frequency distributions of particle size, shown in Fig. 3.

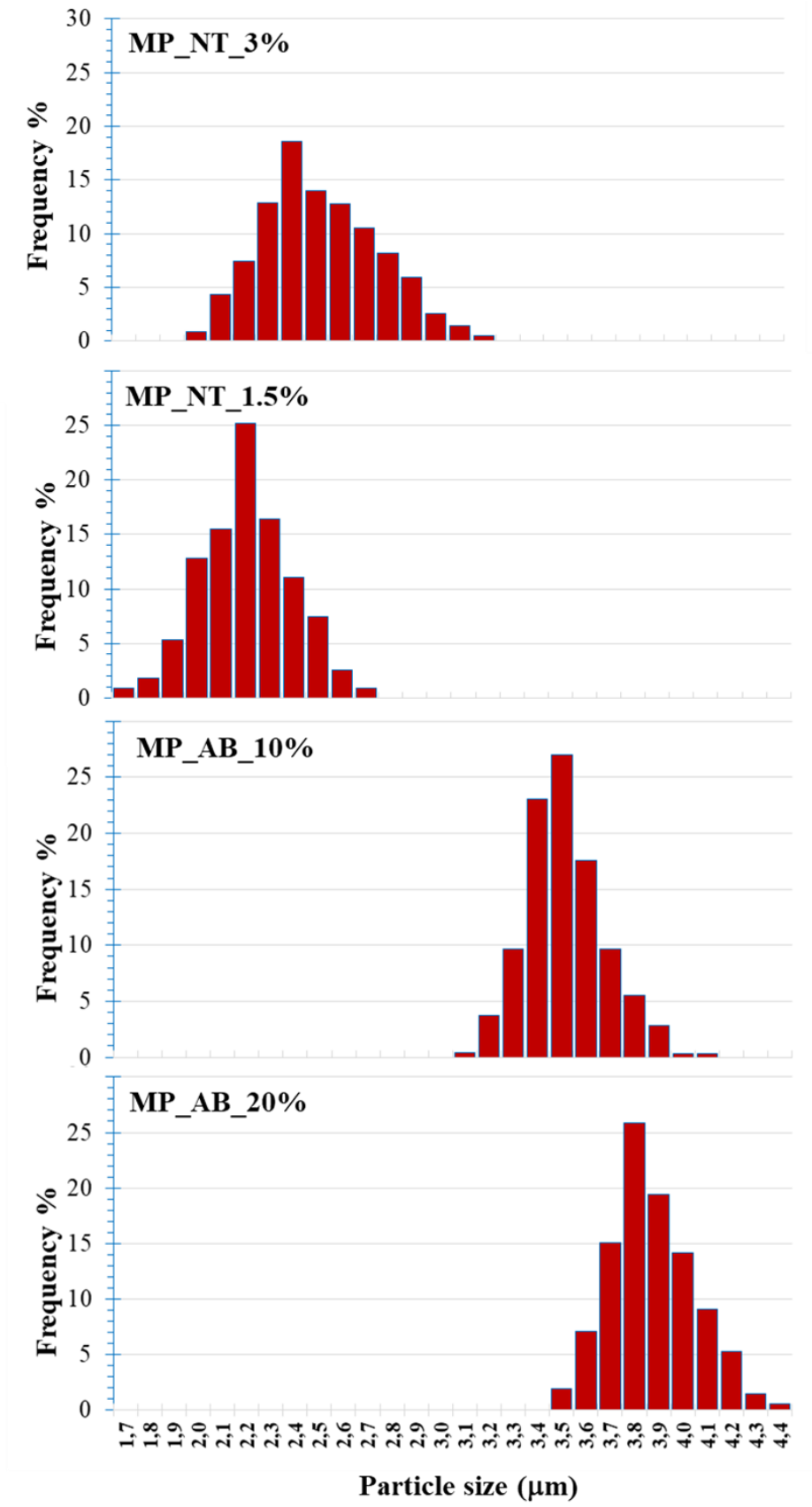

Fig.3. Frequency size distribution of MPs samples.

To have additional information on the surface characteristics, i.e. morphology and roughness, of the MPs surface, an AFM analysis was carried out on both samples (Fig. 4) (see Supporting Information for experimental details).

In particular, a first two-dimensional image with an area of 8 μm x 8 μm was obtained, allowing to appreciate the particle average size. To determine the surface roughness, from the first image at least three portions of particle surface were selected, with an area of 500 nm x 500 nm, and on each image a quadratic polynomial surface was subtracted to mimic the same surface, but spherical and smooth. In this way, the mean square roughness (Rq) value was calculated for each sample, which provides a measure of the regularity of the pores / grooves present on the surface. In the fig. S1 (see Supporting Information section), the vertical fluctuation profiles obtained from the AFM images of the 2D surfaces of all the MP_NT_1.5% and MP_NT_3% samples are shown.

As can be observed in Fig. 4, the particle surface of MP_NT_3% sample showed large "holes", as well as a high Rq value, therefore presenting large lateral fluctuations. On the other hand, at halved copolymer concentration (1.5% wt/vol), the surface is morphologically more regular, as well as the Rq value is significantly reduced compared to MP_NT_3% sample (1.2 nm vs 5.4 nm).

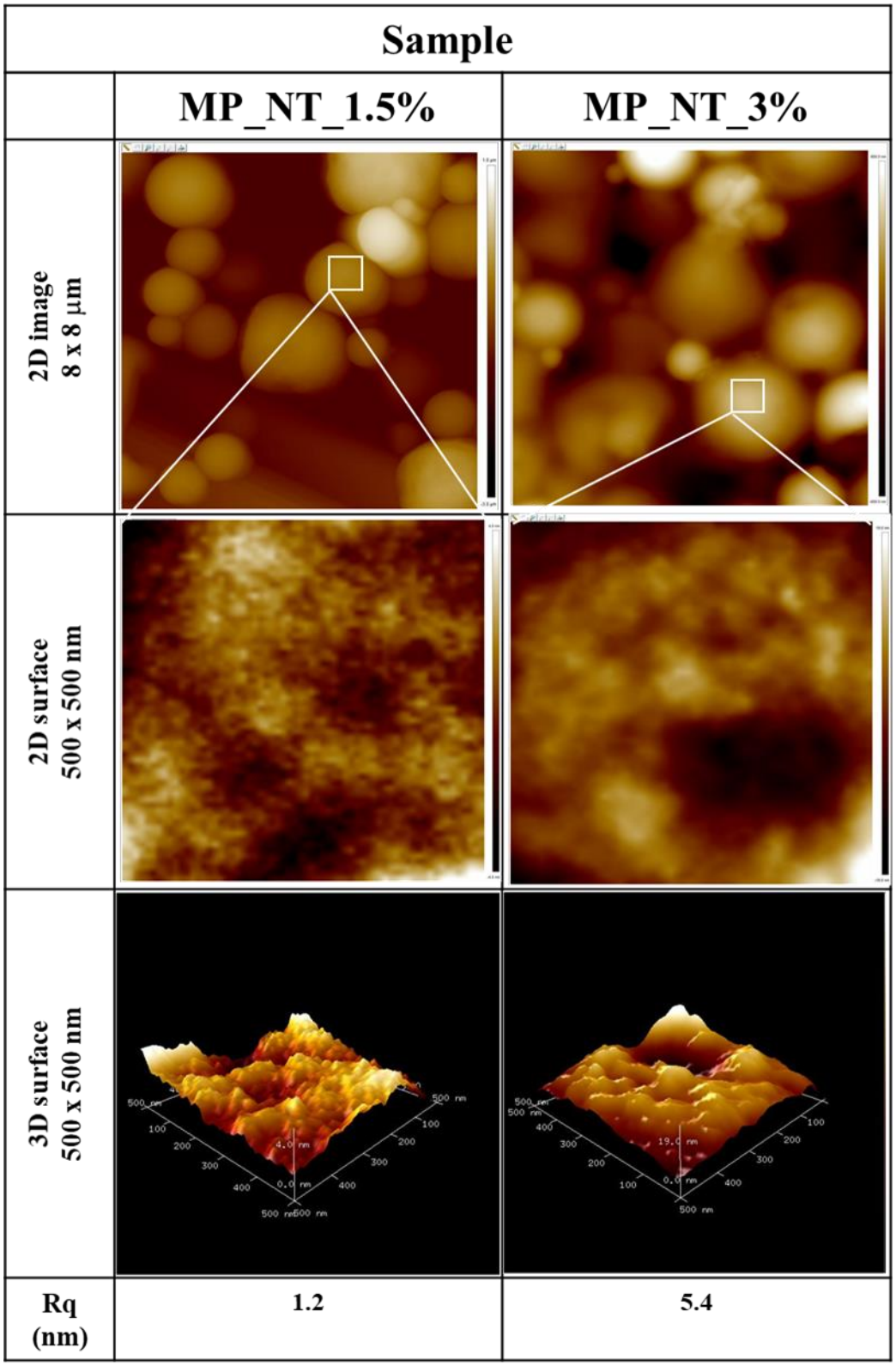

Fig. 4. Representative AFM 2D images, 3D reproduction, Rq of the samples MP_NT_1.5% and MP_NT_3%.

As the MP_NT_1.5% sample shows a regular surface, 1.5% wt/vol was chosen as copolymer concentration in the liquid feed to produce porous MPs by adding ammonium bicarbonate

(AB) at 10 and 20 weight percentage on the copolymer weight in the liquid feed. AB is a gas-evolving salt, which decomposes above 50°C causing carbon dioxide and ammonia gas formation. Its use as a porogen for the production of polymeric microparticles or scaffolds by means of different techniques allows to produce matrices with large pores with extreme ease [14,16]. Therefore, AB was chosen to produce porous MPs, considering that at 60°C it is likely removed directly during the SD process forming pores in the matrix particles [33,34].

Preliminary experiments carried out by a polymeric porogen such as polyethylenglycol (PEG) evidenced that, although a significant increase in size and reduction of tapped density was obtained compared to MP_NT particles, the use of PEG did not determine a significant increase in the surface area, nor differences in the drug release profile compared to that obtained from MP_NT sample (data not shown). Moreover, it made necessary to purify the MPs after production. Therefore, AB is a more suitable choice for the production of MPs via SD.

Here, the porogen was solubilized in MilliQ water and added to the acetonic copolymer dispersion to have a resulting aceton:water vol ratio equal to 39:1. After the SD process, two MP samples were produced: MP_AB_10 and MP_AB_20, respectively, as 10 or 20 weight percentage of AB were added to the liquid feed. The obtained yields were both above 57 wt% with respect to the total weight of the starting components in the spray-dried feed fluid.

The FT-IR analysis demonstrated that the porogen was effectively eliminated during the SD process, being the spectra of the samples perfectly superimposable to that of the sample obtained in the absence of AB (Fig. 5).

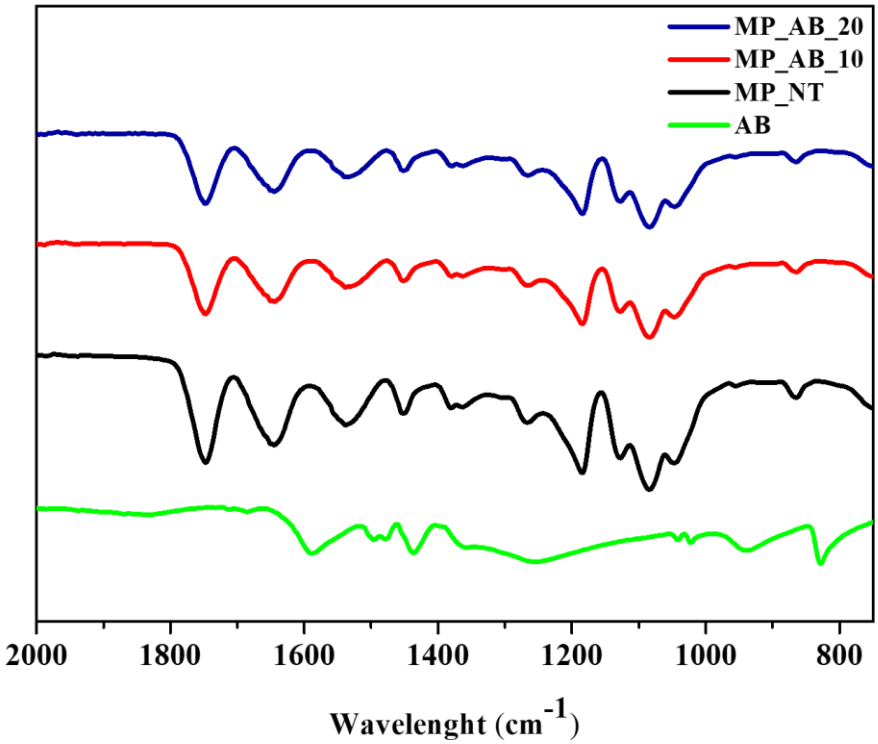

Fig. 5. FT-IR spectra of AB (green line), MP-NT (black line), MP_AB_10 (red line) and MP_AB_20 (blue line) samples.

SEM analysis (Fig. 2) of the MP_AB_10 and MP_AB_20 samples highlights the spherical shape as well as an inhomogeneous matrix for MP_AB_20. The mean size values, obtained also by the image analysis with Imagej software and reported in Table 2, demonstrate that the addition of the porogen in the liquid feed causes a significant increase in the average diameter than that obtained from the copolymer alone. Moreover, as the weight percentage of AB increased, the mean diameter significantly increases.

As for the MP_NT samples, AFM analysis was carried out to the obtained particles to know the effect of the porogen use on the MPs surface characteristics. Obtained images and Rq are reported in Fig. 6.

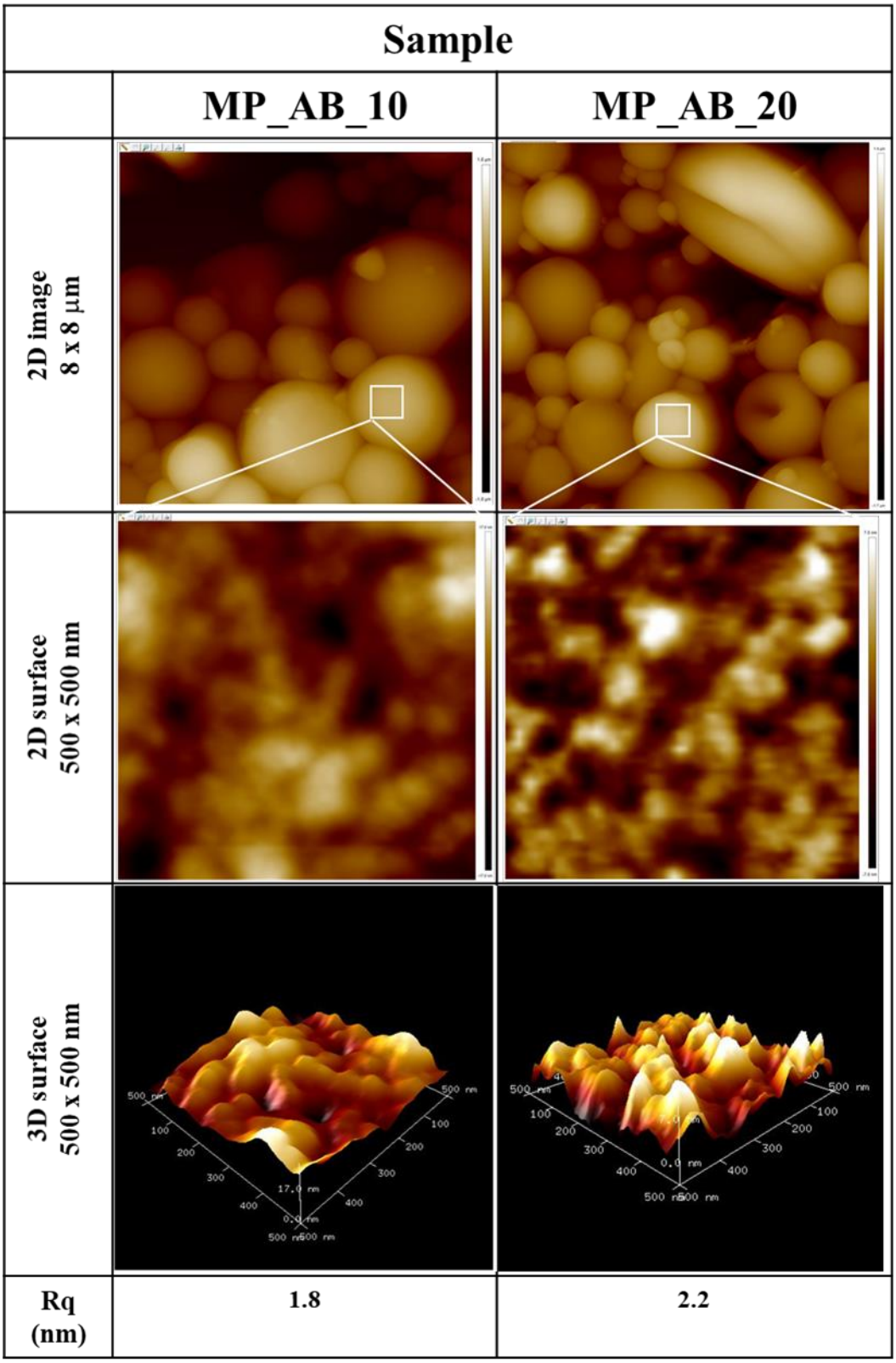

Fig. 6. Representative AFM 2D images, 3D reproduction, Rq of the MP_AB_10 and MP_AB_20 samples.

These revealed a particle surface morphology with clearly visible pores, which increase in number and size as the Ab amount added to the liquid feed of the SD process increases. Furthermore, the surface roughness also increases as the amount of porogen added in the liquid feed (Rq 1.8 nm vs 2.2 nm). In the fig. S1 (see Supporting Information section), the vertical fluctuation profiles obtained from the AFM images of the 2D surfaces of MP_AB_10 and MP_AB_20 samples are shown. Therefore, the addition of AB to the liquid feed affects the surface morphology of the obtained samples, as well as the mean particle size; moreover, the most evident effects are determined at a weight percentage between the porogen and the copolymer equal to 20.

To further investigate the surface characteristics of the obtained MPs, i.e. the surface area and the dimensional distribution of pores present on the particle surface, all samples were characterized by determining the quantity of adsorbed / desorbed gas on the particle surface. In particular, to obtain the specific surface area values of each sample, the Multipoint Brunauer-Emmet-Teller (BET) model was used, while the Barrett, Joyner and Halenda (BJH) model was used to calculate the pore volume and size on the MPs surface. Figure 7 shows the obtained linear isotherms, which show how the volume of adsorbed gas varies as a function of the relative pressure P/P_0 of N_2 at 77K.

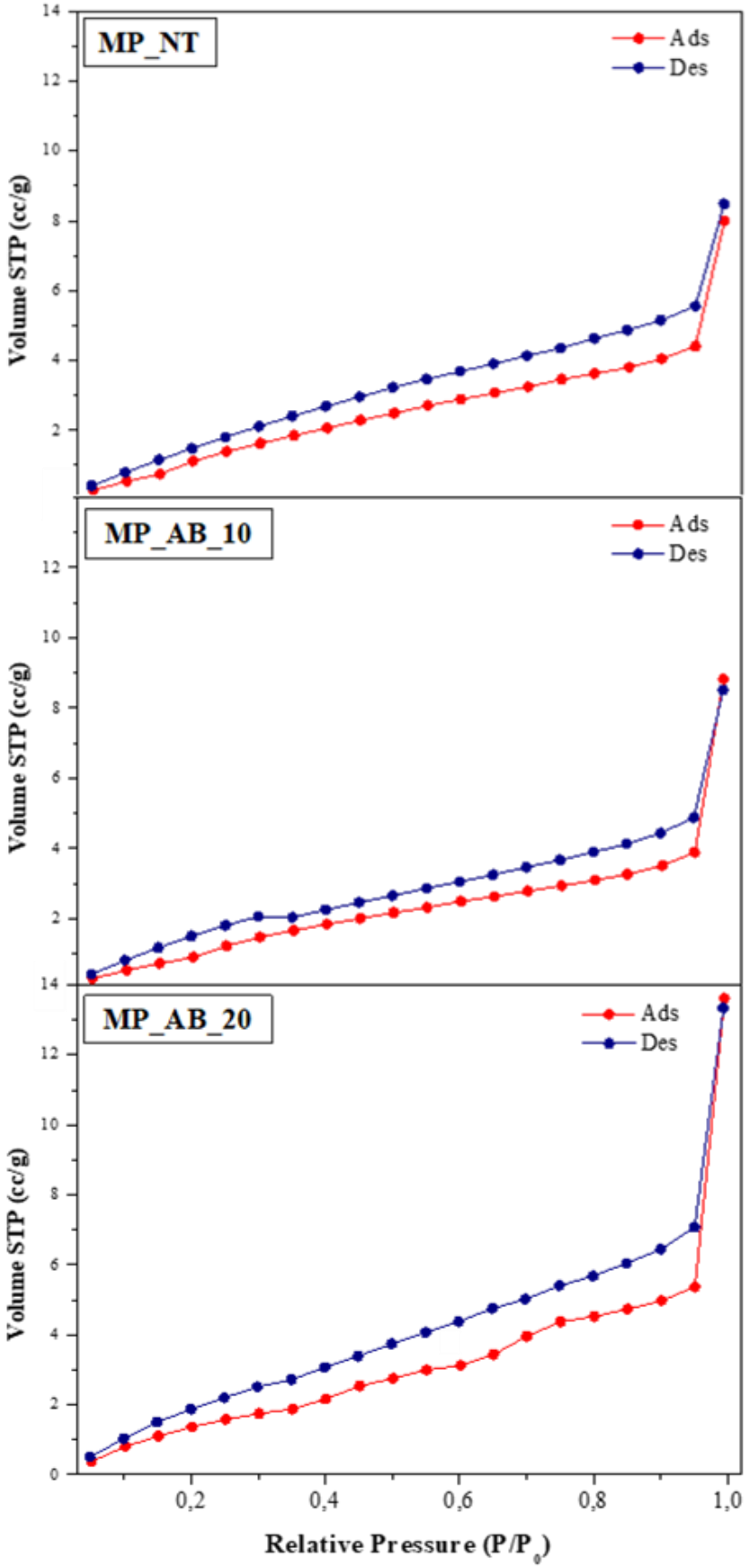

Fig. 7. Representative BET linear isotherms for MP-NT, MP_AB_10 and MP_AB_20 samples.

According to IUPAC, all the obtained isotherms are the type-III, being characterized by a low adsorption of adsorbate at low partial pressure values, which increases at high pressures until P/P_0 reaches the unity. Moreover, a hysteresis loop is present in all the isotherms, showing a different trend of the gas adsorption/desorption profile. The analysis of the obtained data by BET and BJH models gives values of the surface areas, the average size and volume of pores for all the obtained samples (Table 3). In Fig. 8, the pore size distribution on MPs samples are reported as a function of adsorbed gas volume.

Table 3. Data obtained from the Multipoint BET and BJH method analysis. Values represent mean ± SD (n=3).

Sample	**Surface Area (Multipoint BET) (m^2 / g)**	**Surface area of pores (BJH) (m^2 / g)**	**Average pore diameter (nm)**	**Pore volume (cc / g)**
MP_NT	10.184 ± 0.232	10.822 ± 0.403	1.942 ± 0.096	0.015 ± 0.003
MP_AB_10	7.178 ± 0.365	9.378 ± 0.144	2.456 ± 0.126	0.016 ± 0.002
MP_AB_20	9.033 ± 0.502	13.491 ± 0.336	3.060 ± 0.171	0.024 ± 0.004

The surface area values, obtained both by means of the BET and BJH models, show a similar trend. In particular, the MP_NT sample shows the higher surface area values, that can be justified considering the smaller size of these MPs (2.2 ± 0.3μm) compared to those obtained in the presence of porogen. Moreover, the surface area increases as the AB weight percentage in the spray-dried dispersion increases (10 vs 20%), as well as the average diameter and the volume of the pores. In particular, the MP_AB_10 sample shows a slight increase in the pore volume (0.016 vs 0.015 cc/g) as well as in the mean diameter compared to the MP_NT sample (2.456 vs 1.942 nm). On the other hand, the sample that appears significantly different from the others is MP_AB_20, as both the volume occluded by the pores is almost doubled compared to MP_NT (0.024 vs 0.015 cc/g), while it shows two populations of pores with diameters equal to 2.818 and 6.805, respectively. A similar trend was already highlighted elsewhere by using salts or polymers as porogens (i.e. AB or PVP), that is the porosity of polymeric MPs is tunable by the porogen content [14,35]. In particular, Oh and coworkers demonstrated that either the pore size and mean diameter of polylactide-co-glycolide

(PLGA)-based MPs increased with an increase of AB concentration used for their production [14].

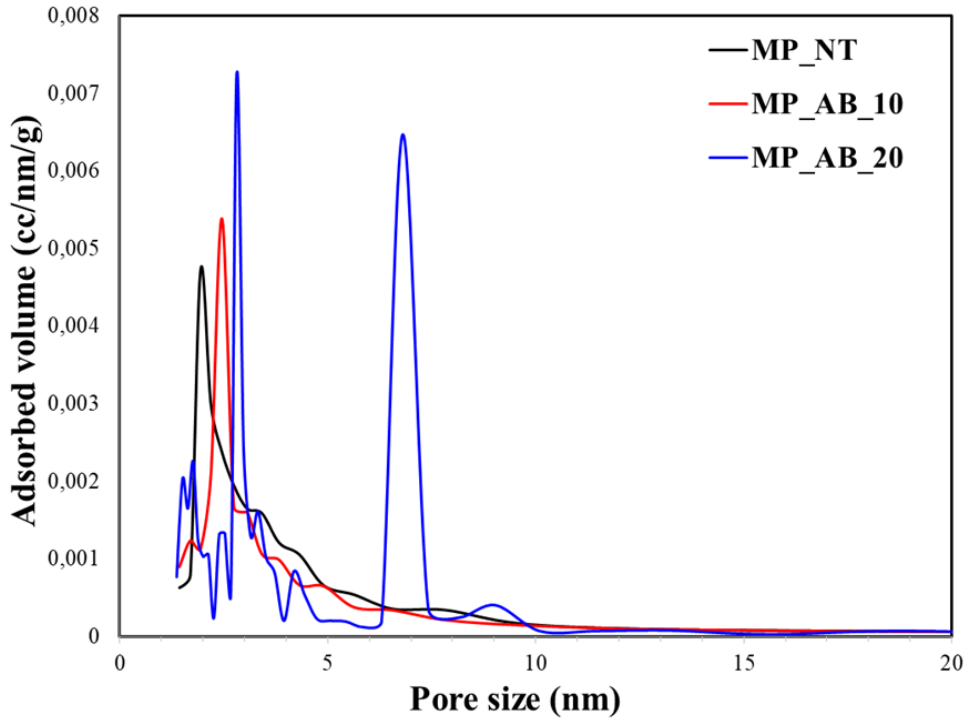

Fig. 8. Representative pore size distribution for each MPs sample (BJH method).

Based on these results, it is expected that even the flow properties, important for adequate inhalation, can be influenced by the highlighted differences between the MP samples.

To evaluate the potential aerodynamic behavior of the obtained MPs after inhalation, the values of tapped density (ρ_{tapp}) and Carr Index (CI) were calculated using the syringe method (Table 4) [17]. As can be seen, the ρ_{tapp} values decrease as the weight percentage of porogen increases in the liquid feed, indicating that the MPs sample becomes less compact due to the formation of pores in the matrices.

Table 4. Values of tapped density (ρ_{tapp}), mean geometric diameter (d_g), theoretical aerodynamic diameter (d_{aer}) values of MP samples. Values represent mean ± SD (n=3).

Sample	**ρ_{tapp} (g/ml)**	**d_g (µm)**	**Theoretical d_{aer} (µm)**	**CI (%)**
MP_NT	0.75 ± 0.03	2.2 ± 0.3	1.9 ± 0.2	49.3 ± 6.3
MP_AB_10	0.54 ± 0.04	3.6 ± 0.5	2.6 ± 0.4	50.0 ± 3.7
MP_AB_20	0.50 ± 0.03	3.8 ± 0.5	2.7 ± 0.2	36.0 ± 4.2

By applying the formula (1) described in the experimental part, the theoretical aerodynamic diameter (d_{aer}) for each MPs sample was calculated. Data show that the use of porogen determines an increase in the MPs size, but at the same time the formation of pores, that causes a reduction in the theoretical d_{aer}. On the other hand, the low d_{aer} value of MP_NT sample, despite having the highest tapped density value, can be explained considering the smallest geometric mean diameter (2.2 μm) used in formula (1). As regards the smoothness of the powder MPs, evaluated by calculating the CI (Table 4), the MP_AB_02 sample shows the best flow properties having the lowest value.

To evaluate the drug deposition and determine the aerodynamic parameters, the samples were tested using the DPI Breezhaler ® connected to the NGI. As concerns the deposition on the NGI stages (Fig. 9), although the MP_AB samples are significantly larger than the MP_NT ones, these had a similar behavior and showed the best aerodynamic properties, being mainly found in the intermediate stages (3 and 4), with a significantly higher deposition of the MP_AB_20 samples.

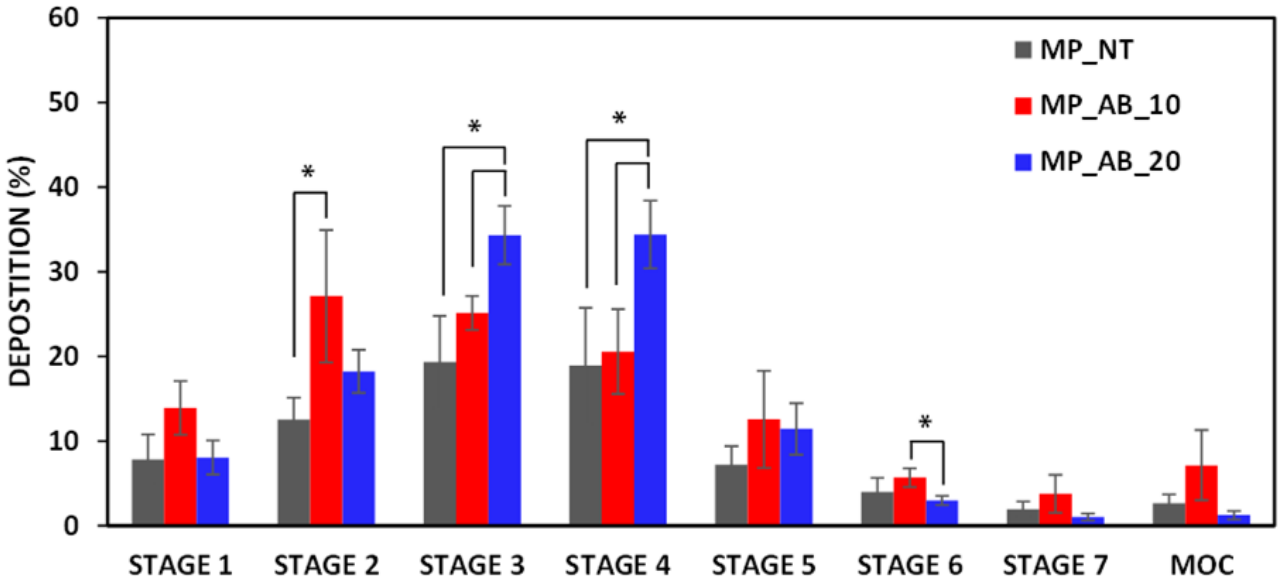

Fig. 9. Deposition of MP samples on the stages of the NGI after testing with Breezhaler ® at a flow rate of 90 L/min (* $p < 0.05$). Values represent mean ± SD (n=3).

Concerning the aerodynamic parameters (Table 5), all the tested samples exhibited high aerosolization efficiency in terms of ED, with values in the range of 69.4 and 69.8 %. The MP_AB_20 showed a slight increase of the FPF% compared to the sample without template,

varying from 11.1 % (MP-NT) to 12.5% (MP_AB_20). Other authors have already reported that the FPF of the MPs increases as a function of the AB amount [36]. Moreover, the MMAD was found almost unvaried to each other (from 2.1 to 2.2 μm) and comparable to the theoretical one, giving a DI lower than unit.

Therefore, it is possible to conclude that the addition of AB determines the formation of larger and less compact matrices thanks to the formation of pores during the SD process and, as a consequence, a modulation of the characteristics of the powder, reducing its density. As concerns the aerodynamic properties, MP_AB show values of MMAD comparable to the theoretical d_{aer}, confirming the excellent flow and aerosolization properties of the obtained particles, therefore suitable for use as inhalable pulmonary carriers of drugs.

Table 5. Aerodynamic parameters of the tested samples: emitted dose (ED%), fine particle dose (FPD), fine particle fraction (FPF), mass median aerodynamic diameter (MMAD), geometric standard deviation (GSD) and dispersibility index (DI). Values represent mean ± SD (n=3).

	MP_NT	**MP_AB_10**	**MP_AB_20**
ED%	69.8 ± 3.0	69.4 ± 2.0	69.5 ± 3.3
FPD (mg)	1.9 ± 0.6	1.4 ± 0.5	2.3 ± 0.2
FPF (%)	11.1 ± 3.6	8.9 ± 2.6	12.5 ± 1.4
MMAD (μm)	2.1 ± 0.1	2.2 ± 0.3	2.2 ± 0.2
GSD	3.3 ± 0.1	3.5 ± 0.1	3.0 ± 0.1
DI	1.1	0.8	0.8

To evaluate as the different surface area and porosity could influence the release kinetics of an entrapped drug, Rapamycin was chosen as model drug. As from our previous studies, we noticed a poor release rate by polymeric matrices of similar composition [37].

Rapamycin is an inhibitor of mTOR (protein kinase that regulates cell growth, proliferation, motility and survival), used orally as an anti-rejection drug in organ transplantation; thanks to its mechanism of action, it is potentially useful for the treatment of lung diseases such as idiopathic pulmonary fibrosis (IPF) and chronic obstructive pulmonary disease (COPD)[38–40].

The average size and tapped density values of obtained Rapamycin-loaded MPs samples were superimposable to the empty ones (data not shown). The Drug Loading (DL%) values were were not significantly different from each other samples and equal to 2.2%, with an Efficiency

of Encapsulation (EE%) of 44 wt%. Other author have reported an EE% below 50 wt% for theoretical DL values equal to 5 wt%, as in this case [34].

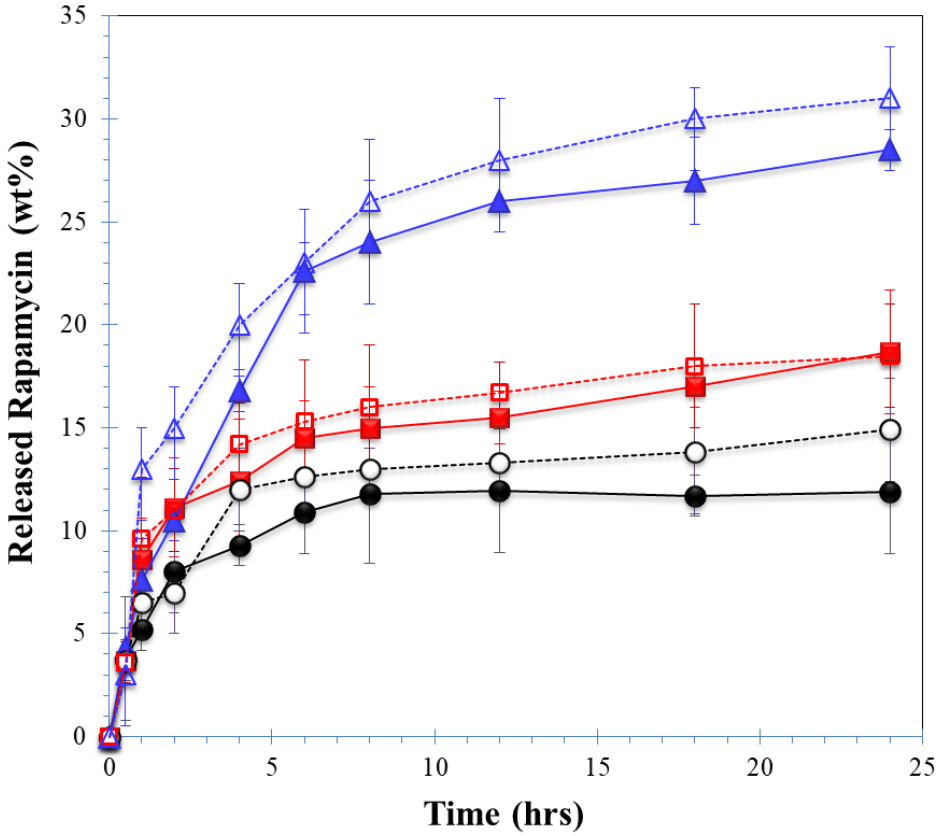

Fig. 10. Rapamycin release profiles from MP_NT (black indicator), MP_AB_10 (red indicator) and MP_AB_20 (blue indicator), in cell medium (full indicator), and in simulated lung fluid (empty indicator). Data represent mean ± SD (n=3).

The drug release profiles (Fig. 10, see Supporting Information for experimental details), show non-significant differences in the amount of drug released from the MP_NT and MP_AB_10 samples up to 12 hours of incubation in both chosen media (cell medium and simulated lung fluid, SLF4) [41]. At incubation times greater than 12 hours in cell medium, the difference becomes significant, reaching values of 11.9 and 18.7% of released drug, respectively, from the MP_NT and MP_AB_10 samples after 24 hours of incubation. On the contrary, the amount of drug released from the MP_NT and MP_AB_10 samples in simulated lung fluid (SLF4), is not statistically significant after 24 hours of incubation, being equal to 14.9 and 18.5% of released drug, respectively. On the other hand, the drug profile released by the MP_AB_20 sample in both media is significantly higher than the other samples after 2 hours

of incubation, reaching the 28.5 and 31.0% of the total loaded amount after 24 hours of incubation, respectively, in cell medium and in SLF4. This result can be explained considering a significant higher surface area and porosity of MP_AB_20 than the other MPs samples.

In literature, there are several evidences that the release rate of drugs loaded into polymeric PLGA-based MPs under sink conditions was porogen concentration dependent (such as AB, PBS or PVP), as the porogen increases the faster release kinetics [14,35,42]. In the same way, a faster release of endosomolytic nanoparticles from PLGA-based MPs was associated to an increase in surface area due to the use of different amount of AB [43].

Moreover, the process of MP production, i.e. the modified emulsion solvent (w/o) evaporation method, as well as the need of MP washing to remove a polymeric porogen, causes a burst effect in the drug release profile [35,44]. The extent and magnitude of the initial burst release seems to depend on the drug present on the MPs surface that dissolved throughout pores and channels, which are most likely formed during the production process and purification process; therefore, the burst effect is also porogen concentration dependent [44].

In the case of our MPs, the drug release burst is absent since the production method via SD and the absence of the need for AB washing from the MPs samples subsequent to the preparation avoids the possible diffusion of the drug towards pores and the particle surface. In all case anyway, these results implies that the release behavior of porous MPs was tunable via adjusting the porogen content.

Therefore, these MPs represent potential carriers for the pulmonary delivery of drugs, being possible to modulate their porosity, which significantly affect properties such as surface area and aerodynamic behavior.

Being these MPs proposed for a potential administration by inhalation route, an in vitro study on 16-HBE cells was assessed. Cytocompatibility of Rapamycin-loaded MPs was evaluated using different concentrations and compared to free drug and empty MPs (at concentration corresponding to drug-loaded samples) after 24 h of incubation (Fig. 11). Both empty and Rapa-loaded MPs have no significant effects on cell viability after 24 h incubation, being the cell viability always higher than 80%, at chosen experimental conditions. On the other hand, the free drug shows a significant cytotoxicity dependent by dose. This difference is due to slow release kinetics of drug from the matrices, leading a lower amount of Rapamycin available to the cells.

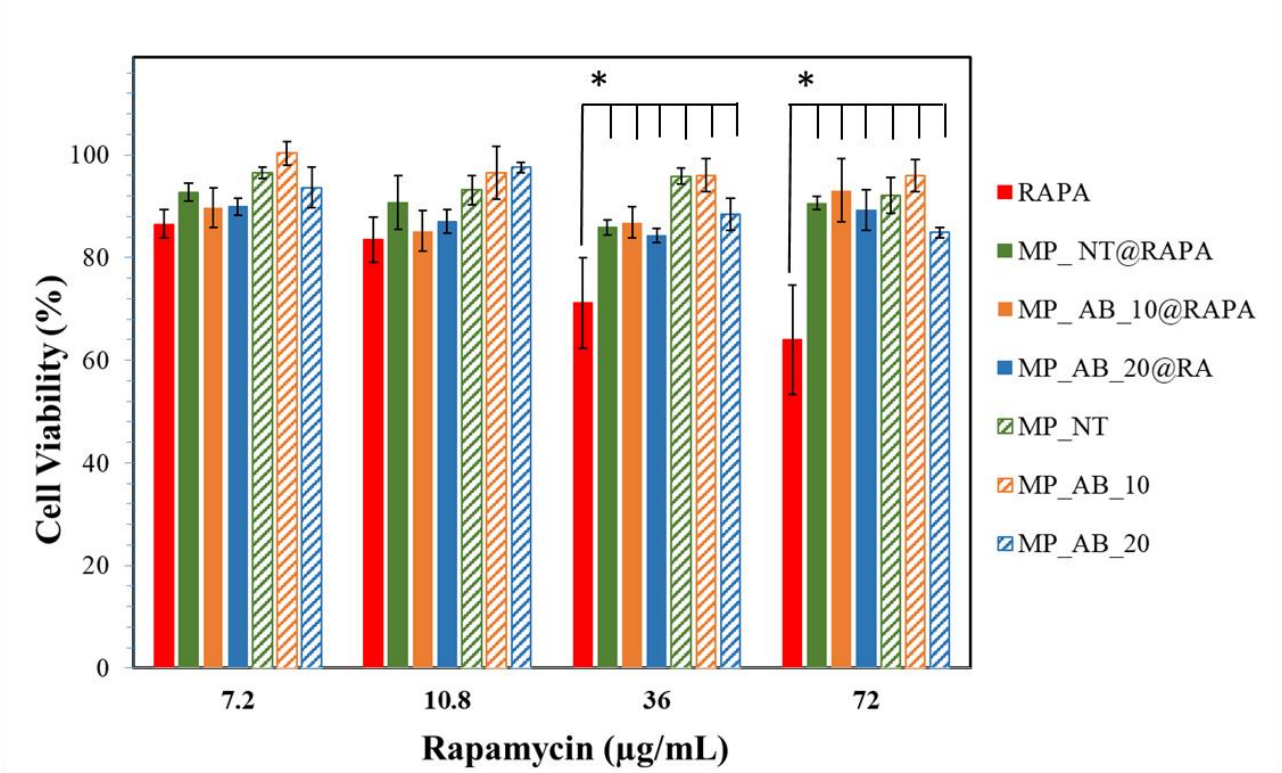

Fig. 11. 16-HBE viability % after incubation in the presence of empty or Rapamycin-loaded MPs in the range 7.2–72 µg/mL, after 24 h of incubation.

Discussion

Inhalable polymeric microparticles (MPs) were produced by spray drying (SD) and proposed for a potential application as drug carriers for the treatment of lung diseases.

These particles were obtained by using as liquid feed of the SD process an acetone/water dispersion of a fluorescent polyaspartamide-polylactide graft copolymer, the PHEA-g-RhB-g-PLA. Ammonium bicarbonate (AB) was added to the liquid feed of the process to modify the microparticle morphology and, consequently, their technological properties (i.e. aerosolization behavior and drug release profile). In particular, it sublimates and decomposes during the SD process, determining the formation of pores in the matrix without the need to be removed by washing in water.

From the mean size analysis of the obtained MPs, it was demonstrated that the use of increasing amount of AB determines an increase in the average diameter compared to the sample obtained without porogen. The atomic force microscopy (AFM) analysis evidenced that the MPs morphology depends on the concentration of PHEA-g-RhB-g-PLA polymer and on the AB amount added in the feed fluid used for their production. In particular, in the absence of porogen, particles with homogeneous surface and reduced roughness are obtained. By contrast, the addition of increasing amounts of the porogen agent determines the formation of more numerous and larger "holes" on the surface, as well as an increase of the roughness and porosity.

The quantification of the adsorbed / desorbed gas on the particle surface indicated that the surface area and porosity of the MPs increases as the porogen agent in the liquid feed increases, showing the higher values of surface area and porosity in the sample obtained with a weight percentage equal to 20. At the same time, the tapped density values of each sample also decreases as the porogen amount added in the feed liquid of the SD process increases. From these data it was possible to calculate the theoretical aerodynamic diameter, which decreases respect to the geometrical diameter as the amount of porogen used increases. Furthermore, the aerodynamic parameters were studied by testing the MPs with a commercial DPI connected to the NGI. The overall results showed that MMAD of the aerosolized MP_NT and MP_AB was approximately 2 μm, that is superimposable on the theoretical d_{aer}.

Furthermore, the advantage of obtaining matrices with different porosity was highlighted by evaluating the release profile of Rapamycin, chosen as model drug, and incorporated into the MPs during the SD process. In particular, the drug release kinetics obtained from the

MP_AB_20 sample was significantly higher, being the quantity of released drug after 24 hours of incubation in SLF4 equal to 31.0% compared to both the MP_NT (14.9%) and MP_AB_10 (18.5%) samples, this result confirms the significantly differences in the matrices obtained by modulating the amount of AB during the production of MP samples.

All matrices, regardless of the amount of AB used for their production and the presence of the incorporated drug, are not very toxic on 16HBE cells compared to the free drug after 24 hours of incubation, demonstrating the biocompatibility of the polymeric matrices and confirming the slow kinetics release of the drug.

Acknowledgments

Authors thank Advanced Technologies Network Center (ATeNCenter) of University of Palermo - Laboratory of Preparation and Analysis of Biomaterials, for scanning electron microscopy and micropore chemoadsorption / physioadsorption Autosorb iQ analyses. Authors thanks Mr. Francesco Paolo Bonomo for technical support.

Appendix A. Supplementary material

Supplementary data to this article can be found online.

References

1. Ang MJY, Chan SY, Goh YY, Luo Z, Lau JW, Liu X. Emerging strategies in developing multifunctional nanomaterials for cancer nanotheranostics. Adv Drug Deliv Rev. 2021;178:113907.
2. Cai SS, Li T, Akinade T, Zhu Y, Leong KW. Drug delivery carriers with therapeutic functions. Adv Drug Deliv Rev. 2021;176:113884.
3. Webber MJ, Pashuck ET. (Macro)molecular self-assembly for hydrogel drug delivery. Adv Drug Deliv Rev. 2021;172:275–95.
4. Mehta PP, Dhapte-Pawar VS. Repurposing drug molecules for new pulmonary therapeutic interventions. Drug Deliv Transl Res. 2021;11:1829–48.
5. Newman SP. Delivering drugs to the lungs: The history of repurposing in the treatment of respiratory diseases. Adv Drug Deliv Rev. 2018;133:5–18.
6. Huang A, Li X, Liang X, Zhang Y, Hu H, Yin Y, et al. Solid-phase synthesis of cellulose acetate butyrate as microsphere wall materials for sustained release of Emamectin benzoate. Polymers (Basel). 2018;10(12):1381.
7. Wang C, Yang J, Han H, Chen J, Wang Y, Li Q, et al. Disulfiram-loaded porous PLGA microparticle for inhibiting the proliferation and migration of non-small-cell lung cancer. Int J Nanomedicine. 2017;12:827–37.
8. Zhang X, Qin L, Su J, Sun Y, Zhang L, Li J, et al. Engineering large porous microparticles with tailored porosity and sustained drug release behavior for inhalation. Eur J Pharm Biopharm. 2020;155(April):139–46.
9. Jeong D, Kang C, Jung E, Yoo D, Wu D, Lee D. Porous antioxidant polymer microparticles as therapeutic systems for the airway inflammatory diseases. J Control Release. 2016;233:72–80.
10. Jain H, Bairagi A, Srivastava S, Singh SB, Mehra NK. Recent advances in the development of microparticles for pulmonary administration. Drug Discov Today. 2020;25(10):1865–72.
11. Carvalho TC, Peters JI, Williams RO. Influence of particle size on regional lung deposition - What evidence is there? Int J Pharm. 2011;406(1–2):1–10.
12. Pulivendala G, Bale S, Godugu C. Inhalation of sustained release microparticles for the targeted treatment of respiratory diseases. Drug Deliv Transl Res. 2020;10(2):339–53.

13. Park S, Kwag DS, Lee UY, Lee DJ, Oh KT, Youn YS, et al. Highly porous poly(lactide-co-glycolide) microparticles for sustained tiotropium release. Polym Adv Technol. 2014;25(1):16–20.
14. Oh YJ, Lee J, Seo JY, Rhim T, Kim SH, Yoon HJ, et al. Preparation of budesonide-loaded porous PLGA microparticles and their therapeutic efficacy in a murine asthma model. J Control Release [Internet]. 2011;150(1):56–62. Available from: http://dx.doi.org/10.1016/j.jconrel.2010.11.001
15. Kim I, Byeon HJ, Kim TH, Lee ES, Oh KT, Shin BS, et al. Doxorubicin-loaded porous PLGA microparticles with surface attached TRAIL for the inhalation treatment of metastatic lung cancer. Biomaterials [Internet]. 2013;34(27):6444–53. Available from: http://dx.doi.org/10.1016/j.biomaterials.2013.05.018
16. Chvatal A, Ambrus R, Party P, Katona G, Jójárt-Laczkovich O, Szabó-Révész P, et al. Formulation and comparison of spray dried non-porous and large porous particles containing meloxicam for pulmonary drug delivery. Int J Pharm [Internet]. 2019;559(January):68–75. Available from: https://doi.org/10.1016/j.ijpharm.2019.01.034
17. Healy AM, McDonald BF, Tajber L, Corrigan OI. Characterisation of excipient-free nanoporous microparticles (NPMPs) of bendroflumethiazide. Eur J Pharm Biopharm. 2008;69(3):1182–6.
18. Carvalho SR, Watts AB, Peters JI, Williams RO. Dry powder inhalation for pulmonary delivery: Recent advances and continuing challenges. Pulm Drug Deliv Adv Challenges. 2015;35–62.
19. Di A, Zhang S, Liu X, Tong Z, Sun S, Tang Z, et al. Microfluidic spray dried and spray freeze dried uniform microparticles potentially for intranasal drug delivery and controlled release. Powder Technol. 2021;379:144–53.
20. Ahookhosh K, Yaqoubi S, Mohammadpourfard M, Hamishehkar H, Aminfar H. Experimental investigation of aerosol deposition through a realistic respiratory airway replica: An evaluation for MDI and DPI performance. Int J Pharm. 2019 Jul;566:157–72.
21. Khalili S, Ghanbarzadeh S, Nokhodchi A, Hamishehkar H. The effect of different coating materials on the prevention of powder bounce in the next generation impactor. Res Pharm Sci. 2018;13(3):283–7.

22. Liao Q, Lam ICH, Lin HHS, Wan LTL, Lo JCK, Tai W, et al. Effect of formulation and inhaler parameters on the dispersion of spray freeze dried voriconazole particles. Int J Pharm. 2020 Jun;584:119444.
23. Yu H, Teo J, Chew JW, Hadinoto K. Dry powder inhaler formulation of high-payload antibiotic nanoparticle complex intended for bronchiectasis therapy: Spray drying versus spray freeze drying preparation. Int J Pharm. 2016 Feb;499(1–2):38–46.
24. Casula L, Lai F, Pini E, Valenti D, Sinico C, Cardia MC, et al. Pulmonary delivery of curcumin and beclomethasone dipropionate in a multicomponent nanosuspension for the treatment of bronchial asthma. Pharmaceutics. 2021 Aug;13(8):1300.
25. Pilcer G, Amighi K. Formulation strategy and use of excipients in pulmonary drug delivery. Int J Pharm. 2010;392(1–2):1–19.
26. Craparo EF, Licciardi M, Conigliaro A, Palumbo FS, Giammona G, Alessandro R, et al. Hepatocyte-targeted fluorescent nanoparticles based on a polyaspartamide for potential theranostic applications. Polymer (Guildf). 2015;70:257–70.
27. Craparo EF, Pitarresi G, Bondi ML, Casaletto MP, Licciardi M, Giammona G. A nanoparticulate drug-delivery system for rivastigmine: Physico-chemical and in vitro biological characterization. Macromol Biosci. 2008;8(3):247–59.
28. Pitarresi G, Palumbo FS, Calabrese R, Craparo EF, Giammona G. Crosslinked hyaluronan with a protein-like polymer: Novel bioresorbable films for biomedical applications. J Biomed Mater Res - Part A. 2008;84(2):413–24.
29. Craparo EF, Porsio B, Bondì ML, Giammona G, Cavallaro G. Evaluation of biodegradability on polyaspartamide-polylactic acid based nanoparticles by chemical hydrolysis studies. Polym Degrad Stab. 2015;119:56–67.
30. Craparo EF, Porsio B, Sardo C, Giammona G, Cavallaro G. Pegylated Polyaspartamide–Polylactide-Based Nanoparticles Penetrating Cystic Fibrosis Artificial Mucus. Biomacromolecules. 2016 Jan 30;17(3):767–77.
31. Cavallaro G, Craparo EF, Sardo C, Lamberti G, Barba AA, Dalmoro A. PHEA-PLA biocompatible nanoparticles by technique of solvent evaporation from multiple emulsions. Int J Pharm. 2015;495(2):719–27.
32. Sosnik A, Seremeta KP. Advantages and challenges of the spray-drying technology for the production of pure drug particles and drug-loaded polymeric carriers. Adv Colloid Interface Sci. 2015;223:40–54.

33. Ghosh Dastidar D, Saha S, Chowdhury M. Porous microspheres: Synthesis, characterisation and applications in pharmaceutical & medical fields. Int J Pharm. 2018;548(1):34–48.
34. Kankala RK, Lin XF, Song HF, Wang S Bin, Yang DY, Zhang YS, et al. Supercritical Fluid-Assisted Decoration of Nanoparticles on Porous Microcontainers for Codelivery of Therapeutics and Inhalation Therapy of Diabetes. ACS Biomater Sci Eng. 2018;4(12):4225–35.
35. Ni R, Muenster U, Zhao J, Zhang L, Becker-Pelster EM, Rosenbruch M, et al. Exploring polyvinylpyrrolidone in the engineering of large porous PLGA microparticles via single emulsion method with tunable sustained release in the lung: In vitro and in vivo characterization. J Control Release [Internet]. 2017;249:11–22. Available from: http://dx.doi.org/10.1016/j.jconrel.2017.01.023
36. Yang Y, Bajaj N, Xu P, Ohn K, Tsifansky MD, Yeo Y. Development of highly porous large PLGA microparticles for pulmonary drug delivery. Biomaterials [Internet]. 2009;30(10):1947–53. Available from: http://dx.doi.org/10.1016/j.biomaterials.2008.12.044
37. Craparo EF, Drago SE, Quaglia F, Ungaro F, Cavallaro G. Development of a novel rapamycin loaded nano- into micro-formulation for treatment of lung inflammation. Drug Deliv Transl Res [Internet]. 2022;12:1859–72. Available from: https://doi.org/10.1007/s13346-021-01102-5
38. Wang Y, Liu J, Zhou JS, Huang HQ, Li ZY, Xu XC, et al. MTOR Suppresses Cigarette Smoke–Induced Epithelial Cell Death and Airway Inflammation in Chronic Obstructive Pulmonary Disease. J Immunol. 2018;200(8):2571–80.
39. Mitani A, Ito K, Vuppusetty C, Barnes PJ, Mercado N. Restoration of corticosteroid sensitivity in chronic obstructive pulmonary disease by inhibition of mammalian target of rapamycin. Am J Respir Crit Care Med. 2016;193(2):143–53.
40. Ko JH, Yoon SO, Lee HJ, Oh JY. Rapamycin regulates macrophage activation by inhibiting NLRP3 inflammasome-p38 MAPK-NFκB pathways in autophagy- and p62-dependent manners. Oncotarget. 2017;8(25):40817–31.
41. Marques MRC, Loebenberg R, Almukainzi M. Simulated biologic fluids with possible application in dissolution testing. Dissolution Technol. 2011;15–28.
42. Su X, Gupta I, Jonnalagadda US, Kwan JJ. Complementary Effects of Porosigen and

Stabilizer on the Structure of Hollow Porous Poly(lactic-co-glycolic acid) Microparticles. ACS Appl Polym Mater. 2020;2(8):3696–703.

43. Garland KM, Sevimli S, Kilchrist K V., Duvall CL, Cook RS, Wilson JT. Microparticle Depots for Controlled and Sustained Release of Endosomolytic Nanoparticles. Cell Mol Bioeng. 2019;12(5):429–42.

44. Park K, Otte A, Sharifi F, Garner J, Skidmore S, Park H, et al. Formulation composition, manufacturing process, and characterization of poly(lactide-co-glycolide) microparticles. J Control Release [Internet]. 2021;329(October 2020):1150–61. Available from: https://doi.org/10.1016/j.jconrel.2020.10.044